Atmos. Chem. Phys., 14, 12023–12030, 2014
www.atmos-chem-phys.net/14/12023/2014/
doi:10.5194/acp-14-12023-2014

Atmospheric Chemistry and Physics
Open Access

Methane sulfonic acid-enhanced formation of molecular clusters of sulfuric acid and dimethyl amine

N. Bork[1,2], **J. Elm**[2], **T. Olenius**[1], **and H. Vehkamäki**[1]

[1]University of Helsinki, Department of Physics, Division of Atmospheric Sciences, P. O. Box 64, 00014 Helsinki, Finland
[2]University of Copenhagen, Department of Chemistry, Universitetsparken 5, 2100, Copenhagen, Denmark

Correspondence to: N. Bork (nicolai.bork@helsinki.fi)

Received: 10 June 2014 – Published in Atmos. Chem. Phys. Discuss.: 14 July 2014
Revised: 18 September 2014 – Accepted: 21 September 2014 – Published: 17 November 2014

Abstract. Over oceans and in coastal regions, methane sulfonic acid (MSA) is present in substantial concentrations in aerosols and in the gas phase. We present an investigation into the effect of MSA on sulfuric acid- and dimethyl amine (DMA)-based cluster formation rates. From systematic conformational scans and well-tested ab initio methods, we optimise the structures of all MSA_x $(H_2SO_4)_yDMA_z$ clusters where $x + y \leq 3$ and $z \leq 2$. The resulting thermodynamic data are used in the Atmospheric Cluster Dynamics Code, and the effect of MSA is evaluated by comparing ternary MSA–H_2SO_4–DMA cluster formation rates to binary H_2SO_4–DMA cluster formation rates. Within the range of atmospherically relevant MSA concentrations, we find that MSA may increase cluster formation rates by up to 1 order of magnitude, although typically, the increase will be less than 300 % at 258 K, less than 100 % at 278 K and less than 15 % at 298 K. The results are rationalised by a detailed analysis of the main growth paths of the clusters. We find that MSA-enhanced clustering involves clusters containing one MSA molecule, while clusters containing more than one MSA molecule do not contribute significantly to the growth.

1 Introduction

One of the least understood micro-physical processes in the atmosphere is the conversion of low volatile gaseous molecules into an aerosol particle. Aerosol particles are a major source of cloud condensation nuclei, and aerosol formation represents one of the largest uncertainties in climate and cloud models (Solomon et al., 2007; Kazil et al., 2010; Pierce and Adams, 2009). Despite recent advances in theory and instrumentation, the chemical composition of the molecular clusters forming the seeds for the thermally stable aerosol particles remains highly uncertain at most locations.

The decisive importance of sulfuric acid for atmospheric aerosol formation is well established, but within the last decades it has become evident that at least one, but probably more, stabilising species participate as well (Weber et al., 1996; Almeida et al., 2013). Nitrogenous bases, most efficiently dimethyl amine (DMA), and highly oxidised organic compounds are known to enhance sulfuric acid-based aerosol formation. However, at locations where nitrogenous bases are sparse, other species may contribute significantly.

Methane sulfonic acid (MSA) is the simplest organosulfate, and is a well-known oxidation product of dimethylsulfide. Over oceans and in coastal regions, gaseous MSA is present in concentrations of about 10 to 50 % of the gaseous sulfuric acid (H_2SO_4) concentration (Berresheim et al., 2002; Huebert et al., 1996), although MSA / H_2SO_4 ratios of up to 250 % have been reported (Davis et al., 1998). Similarly, in sub-µm aerosol particles, MSA is typically found in concentrations of 5 to 30 % of the sulfate concentrations (Ayers et al., 1991; Huebert et al., 1996; Kerminen et al., 1997), although MSA / sulfate ratios of around 100 % have been reported in aerosols smaller than 0.2 µm (Facchini et al., 2008). It is generally accepted that much particulate MSA originates from surface oxidation of dimethyl sulfoxide (DMSO) and methane sulfinic acid (MSIA) (Davis et al., 1998; Barnes et al., 2006). However, in a recent study by

Dall'Osto et al. (2012), gaseous MSA concentrations were found to decrease during marine particle formation events, suggesting that MSA may contribute to growth and possibly formation of the initial molecular clusters seeding aerosol formation.

Several laboratory and theoretical studies have attempted to explain these observations and determine at which state MSA enters the aerosol particle. Earlier studies have often used classical nucleation theory to predict or reproduce particle formation rates of various mixtures of H_2SO_4, MSA and water, generally finding that MSA is of minor importance (Wyslouzil et al., 1991; Napari et al., 2002; Van Dingenen and Raes, 1993). Later studies by Dawson et al. (2012) and Bzdek et al. (2011), combining flow tube experiments and ab initio calculations, found that water and nitrogenous bases enhanced MSA-based aerosol formation and that amines are more efficient than ammonia, and recently, Dawson et al. (2014) found that trimethylamine was susceptible to substitution by both methylamine and DMA. Furthermore, Dall'Osto et al. (2012) used quantum chemical calculations, considering the molecular clusters containing up to two acids and one DMA molecule, to support the hypothesis that MSA, H_2SO_4 and DMA could co-exist in newly formed molecular clusters.

These studies have prompted a more rigorous ab initio based evaluation of whether MSA contributes to aerosol formation or mainly enters the aerosol during growth. This study targets the enhancing effect of MSA on sulfuric acid–DMA-based cluster formation. Via systematic conformational searches, we have obtained minimum free energy structures of clusters of composition $MSA_x(H_2SO_4)_yDMA_z$ where $x + y \leq 3$ and $z \leq 2$. The corresponding thermodynamic data are used in the Atmospheric Cluster Dynamics Code (ACDC) (McGrath et al., 2012; Olenius et al., 2013), whereby the enhancing effect of MSA is obtained by comparing ternary MSA–H_2SO_4–DMA to binary H_2SO_4–DMA-based cluster formation rates.

The clusters studied in this work do not contain water molecules, due to the considerable additional computational effort required to obtain the necessary thermodynamic data. Hydration can be expected to stabilise weakly bound clusters more than strongly bound clusters, and it is therefore conceivable that we will underestimate the contribution from some of the minor growth pathways. However, since DMA is a much stronger base than water, hydration is not likely to have a significant effect on the stability of clusters containing DMA. Therefore, the main growth pathways and growth rates are unlikely to change significantly due to hydration. See e.g. Almeida et al. (2013) and Henschel et al. (2014) for further discussion.

Table 1. Comparison of various computational approaches for calculating Gibbs free-binding energies. Unless otherwise stated, the basis set is 6-311++G(3df,3pd). F12 is shorthand for CCSD(T)-F12/VDZ-F12. Values in kcal mol^{-1}.

Method	Gibbs free-binding energy $H_2SO_4 + DMA$	$MSA + DMA$
M06-2X	−11.26	−7.42
B3LYP	−8.71	−4.59
PW91	−11.44	−7.75
ωB97X-D	−11.96	−8.98
MP2	−13.70	−10.84
F12//M06-2X	−11.72	−8.19
F12//B3LYP	−11.96	−8.57
F12//PW91	−12.07	−8.74
F12//ωB97X-D	−11.97	−9.33
F12//MP2	−11.99	−9.36
RI-MP2/AV(T+d)Z// RI-MP2/AV(D+d)Z	−12.49[1]	−9.29[1]
RI-MP2/AV(T+d)Z// BLYP/DZP	−15.57 [2]	
RI-CC2/AV(T+d)Z// B3LYP/CBSB7	−15.40 [3]	
PW91	−11.38 [4]	

References: [1] Dall'Osto et al. (2012), [2] Loukonen et al. (2010), [3] Ortega et al. (2012), [4] Nadykto et al. (2011).

2 Computational details

2.1 Ab initio calculations

The most critical parameters in cluster growth models are the cluster-binding free energies, since the evaporation rate depends exponentially on these. At present, density functional theory (DFT) and second-order Møller–Plesset perturbation theory (MP2) are the most popular ab initio methods for calculating the thermodynamics of molecular clusters. It is often mentioned that average uncertainties are of the order of 1 kcal mol^{-1}, but depending on the specific system and method, uncertainties may be significantly larger. Therefore, careful testing and validation should precede each study, which we will discuss in the following.

Since acid–base clustering is considered one of the fundamental processes driving aerosol formation, we have tested the performance of four commonly used DFT functionals and MP2, comparing these to previously published data. Also, the effect of electronic energy corrections from high-level coupled cluster calculations is tested. The basis set effects have previously been found to be much less significant, provided that a basis set of at least triple-ζ quality is used (Bork et al., 2014a). In this study, we use the 6-311++G(3df,3pd) (Francl et al., 1982; Clark et al., 1983) basis set in all DFT and MP2 calculations.

Table 2. Testing the effect of CCSD(T)-F12/VDZ-F12 electronic energy corrections to M06-2X/6-311++G(3df,3pd) Gibbs free energy changes of the indicated reactions. Values in kcal mol^{-1}.

Reaction	Gibbs free-binding energy F12//M06-2X	M06-2X	$\Delta_{\text{F12-DFT}}$
DMA + H_2SO_4	−11.72	−11.26	0.46
DMA + MSA	−8.19	−7.42	0.77
H_2SO_4 + H_2SO_4	−7.07	−8.38	−1.31
H_2SO_4 + MSA	−8.56	−10.70	−2.14
MSA + MSA	−7.53	−9.07	−1.54

From the first and second sections of Table 1, we see that the CCSD(T)-F12/VDZ-F12 electronic energy corrections significantly reduce the scatter of the data. This suggests that the thermal and zero-point vibrational terms are well produced by the four DFT functionals and MP2, and that the main errors are associated with the electronic energies. Also, the data reveal that amongst the tested methods, the M06-2X, ωB97X-D and PW91 density functionals perform well, whereas B3LYP performs poorly in systems representative of clustering by H_2SO_4 and MSA with DMA.

In several recent studies (Bork et al., 2014a, b; Leverentz et al., 2013; Elm et al., 2012, 2013b), the M06-2X functional (Zhao and Truhlar, 2008) has been shown to be amongst the most reliable and accurate density functionals with respect to binding free energies of molecular clusters. Therefore, its performance for the present systems was investigated in greater detail. Table 2 shows the effect of a CCSD(T)-F12a/VDZ-F12 single-point electronic energy correction on the M06-2X Gibbs free energy for five relevant reactions. For the formation of the DMA · H_2SO_4 and DMA · MSA complexes, a slight underestimation is observed, in agreement with previous studies of similar systems (Bork et al., 2014a; Elm et al., 2012, 2013b). For the MSA · H_2SO_4, $(H_2SO_4)_2$ and MSA_2 complexes, the DFT values are seen to overestimate the Gibbs free energies of formation by up to 2.14 kcal mol^{-1}. No reliable representative experimental data exist for comparison of acid–acid cluster binding energies. However, the binding energy of $(H_2SO_4)_2$ has been investigated by Ortega et al. (2012), using MP2 for up to quintuple ζ basis sets, also including anharmonic and relativistic effects, arriving at a value of −7.91 kcal mol^{-1}. This indicates that the apparent overbinding of the M06-2X functional is less severe than 2 kcal mol^{-1} and that M06-2X-based errors in binding energies of molecular clusters with both acid–acid and acid–base bonds will tend to cancel out rather than accumulate.

All DFT and MP2 geometry optimisations and frequency calculations are performed using Gaussian 09 (revision B.01, http://www.gaussian.com), and all CCSD(T)-F12 calculations are performed using Molpro (version 2012.1, http://www.molpro.net).

In addition to an appropriate computational method, a second prerequisite for obtaining correct cluster-binding free energies is to obtain the global minimum energy structures. In this study, we employ a systematic sampling technique initiated by 1000 auto-generated guess structures, pre-optimised using the PM6 semi-empirical method (Stewart, 2007). The up to 100 best-guess structures are refined further using M06-2X/6-311++G(3df,3pd). For full details of the sampling technique, we refer the reader to our previous investigations (Elm et al., 2013c, a). Additionally, guess structures for all cluster compositions were manually constructed based on previously published $(H_2SO_4)_x DMA_y$ and $(H_2SO_4)_x(NH_3)_y$ structures (Nadykto et al., 2011; Ortega et al., 2012). In several cases, this led to structures identical to the above-mentioned systematic sampling, but in no cases did the manual approach lead to improved binding energies compared to the systematic approach.

2.2 Cluster growth model

The resulting thermodynamic data were studied with the Atmospheric Cluster Dynamics Code (ACDC) kinetic model (McGrath et al., 2012; Olenius et al., 2013). The code solves the time evolution of molecular cluster concentrations for a given set of clusters and ambient conditions, considering all possible collision and fragmentation processes. In this study, ACDC is used to find the steady state of the cluster distribution at given concentrations of MSA, H_2SO_4 and DMA. The collision rate coefficients are calculated as hard-sphere collision rates, and the evaporation rate coefficients are calculated from the Gibbs free energies of formation according to a detailed balance.

As the vapour-phase concentrations of MSA and H_2SO_4 are generally measured with chemical ionisation mass spectrometry (CIMS), the atmospheric concentrations reported in the literature are likely to include contributions from acid molecules clustered with bases, in addition to the bare acid monomer (Kupiainen-Määttä et al., 2013). Therefore, the acid concentrations in ACDC (both MSA and H_2SO_4) are defined as the sum of all clusters consisting of one acid molecule and any number of DMA molecules. An external sink with a loss rate coefficient of 2.6×10^{-3} s^{-1}, corresponding to coagulation onto pre-existing larger particles, is used for all clusters (Dal Maso et al., 2008). Testing showed that variations in this value between 10^{-3} s^{-1} and 5×10^{-3} s^{-1} did not affect the main conclusions of this study (Supplement Fig. S1).

When a collision leads to a cluster that is larger than the simulated system, the cluster is allowed to grow out if it contains at least three acid and three base molecules, since these compositions are assumed to be along the main growth path. The probability of a three acid–three base cluster growing further vs. re-evaporating back into the system was investigated by also optimising the MSA–$(H_2SO_4)_2$–DMA_3 clus-

ter. At $T = 298\,\mathrm{K}$, for example, the reaction

$$\mathrm{MSA(H_2SO_4)_2DMA_3} \leftrightarrow \mathrm{MSA(H_2SO_4)_2DMA_2} + \mathrm{DMA}$$

has $\Delta G^{\circ}_{298\,\mathrm{K}} = 14.5\,\mathrm{kcal\,mol^{-1}}$, corresponding to an evaporation rate of $4.3 \times 10^{-1}\,\mathrm{s^{-1}}$ which can be compared to a collision rate with another DMA or H_2SO_4 molecule of $8.4 \times 10^{-2}\,\mathrm{s^{-1}}$ or $5.7 \times 10^{-4}\,\mathrm{s^{-1}}$, respectively ($[\mathrm{DMA}] = 10^8\,\mathrm{molecules\,cm^{-3}}$ and $[\mathrm{H_2SO_4}] = 10^6\,\mathrm{molecules\,cm^{-3}}$). At $T = 258\,\mathrm{K}$, $\Delta G^{\circ}_{258\,\mathrm{K}} = 16.1\,\mathrm{kcal\,mol^{-1}}$, and the evaporation rate of $4.4 \times 10^{-4}\,\mathrm{s^{-1}}$ is much lower compared to collision rates with DMA or H_2SO_4 of $7.8 \times 10^{-2}\,\mathrm{s^{-1}}$ or $5.3 \times 10^{-4}\,\mathrm{s^{-1}}$. This reveals that, depending on the conditions, evaporation of three acid and three base clusters can be significant, and that larger clusters than considered in this study should be included for quantitative assessments of formation rates of nanometre-sized MSA–H_2SO_4–DMA-based particles, in particular at higher temperatures. Our analysis is therefore restricted to formation rates of three acid–three base molecular clusters.

Cluster types outside the simulation box not containing at least three acids and at least three base molecules are considered unstable and hence much more likely to shrink by evaporations rather than being stabilised by another collision. Therefore, these types of clusters are brought back into the simulation by monomer evaporations. In the case that the evaporating molecules are excess acid, the first evaporating molecule is assumed to be MSA, since it is a weaker acid than H_2SO_4. From these simulations, we determine the formation rate of clusters that grow out of the system, and track the main growth routes by following the flux through the system (Olenius et al., 2013).

3 Results

3.1 Structures and thermodynamics

Structures and thermodynamic data for all of the most stable $\mathrm{MSA}_x(\mathrm{H_2SO_4})_y\mathrm{DMA}_z$ clusters, where $x + y \leq 3$ and $z \leq 2$, are given as the Supplement. These clusters share several structural features. In all cases where the number of base molecules does not exceed the number of acid molecules (MSA or H_2SO_4), the DMA moiety is protonated, but in none of the clusters is SO_4^{2-} found. In most clusters containing both H_2SO_4 and MSA, H_2SO_4 is more acidic than MSA. However, in a few cases, including the most stable $H_2SO_4 \cdot \mathrm{MSA} \cdot \mathrm{DMA}$ cluster, deprotonated MSA and doubly protonated H_2SO_4 are seen in the same cluster (Fig. 1a). This is in accordance with the findings of Dall'Osto et al. (2012). Another common feature is the monolayer-like rather than bulk-like structures of even the largest clusters investigated, e.g. MSA$-(H_2SO_4)_2-$DMA$_3$ (Fig. 1b). This tendency has been seen in other studies of similar systems, e.g. H_2SO_4–DMA-based clusters (Ortega et al., 2012) and HSO_4^-–H_2SO_4–NH_3-based clusters (Herb et al., 2012). This

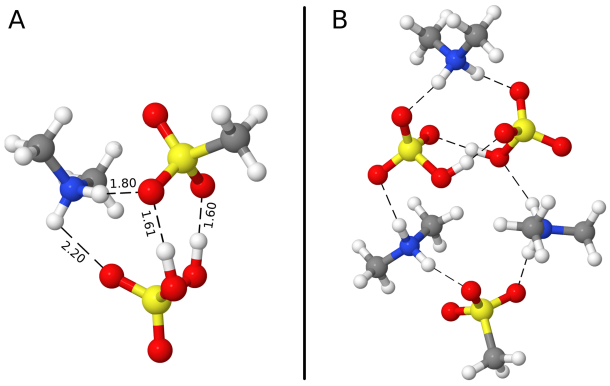

Figure 1. A: Most stable configuration of the $\mathrm{MSA} \cdot \mathrm{H_2SO_4} \cdot \mathrm{DMA}$ cluster. The lengths of the hydrogen bonds are given in Å. In this cluster, MSA is a stronger acid than H_2SO_4. B: Configuration of the $\mathrm{MSA} \cdot (\mathrm{H_2SO_4})_2 \cdot \mathrm{DMA_3}$ cluster. As with all investigated clusters, the most stable structure is more monolayer-like than bulk-like. The hydrogen bonds are shown as dashed lines.

is opposite to clusters containing several water molecules, where bulk-like H_2O structures tend to be more stable (Bork et al., 2013, 2011).

It is well known that strong acids and strong bases tend to form strong hydrogen bonds and more stable clusters than weaker acids and bases. Since MSA is a weaker acid than H_2SO_4, it is expected that the $\mathrm{MSA} \cdot \mathrm{DMA}$ binding energy will be lower than the $\mathrm{H_2SO_4} \cdot \mathrm{DMA}$ binding energy (Table 2). It is, on the other hand, surprising that the $\mathrm{MSA} \cdot \mathrm{H_2SO_4}$ bond is at least $1.5\,\mathrm{kcal\,mol^{-1}}$ stronger than the $\mathrm{H_2SO_4} \cdot \mathrm{H_2SO_4}$ bond, and that the $\mathrm{MSA} \cdot \mathrm{MSA}$ bond is at least $0.5\,\mathrm{kcal\,mol^{-1}}$ stronger than the $\mathrm{H_2SO_4} \cdot \mathrm{H_2SO_4}$ bond. In larger clusters, H_2SO_4 is, however, significantly more stabilised compared to MSA, and, besides the MSA dimer, clusters containing more than one MSA molecule are less stable than their corresponding H_2SO_4-containing analogues (Table S1).

3.2 Clustering enhancements

To analyse the clustering abilities of MSA, a series of ACDC simulations based on these thermodynamics were performed under varying conditions. As a first measure, the binary cluster formation rate of MSA and DMA was compared to those of H_2SO_4 and DMA under similar conditions, i.e. the ratio

$$r_1 = \frac{J([\mathrm{H_2SO_4}] = 0,\ [\mathrm{MSA}] = x,\ [\mathrm{DMA}] = y)}{J([\mathrm{H_2SO_4}] = x,\ [\mathrm{MSA}] = 0,\ [\mathrm{DMA}] = y)}, \qquad (1)$$

where J denotes the cluster formation rate under the indicated conditions.

This was calculated for three temperatures (258, 278 and 298 K) spanning the boundary layer to the lower half of the troposphere, and x in the range from 10^5 to $2 \times 10^6\,\mathrm{molecules\,cm^{-3}}$, corresponding to typical H_2SO_4 and MSA concentrations as described in the introduction.

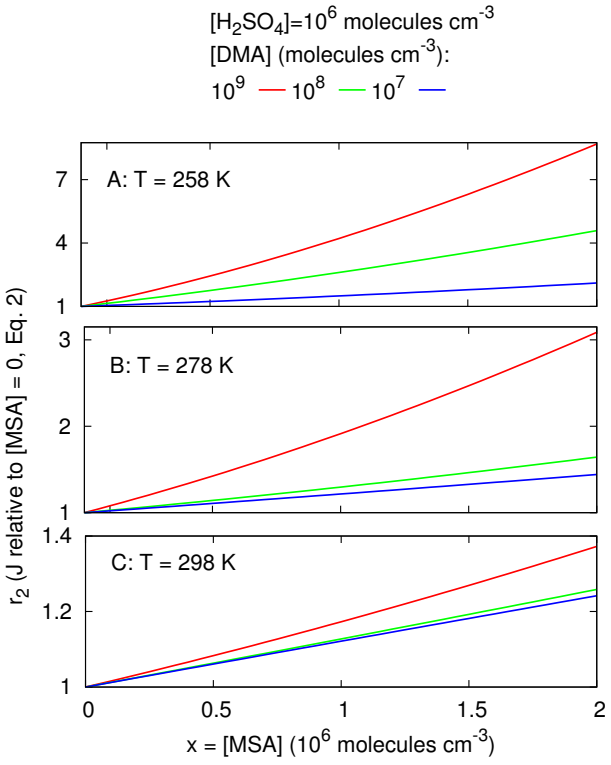

Figure 2. MSA–H_2SO_4–DMA-based particle formation rates at varying MSA concentrations relative to [MSA] = 0 (Eq. 2).

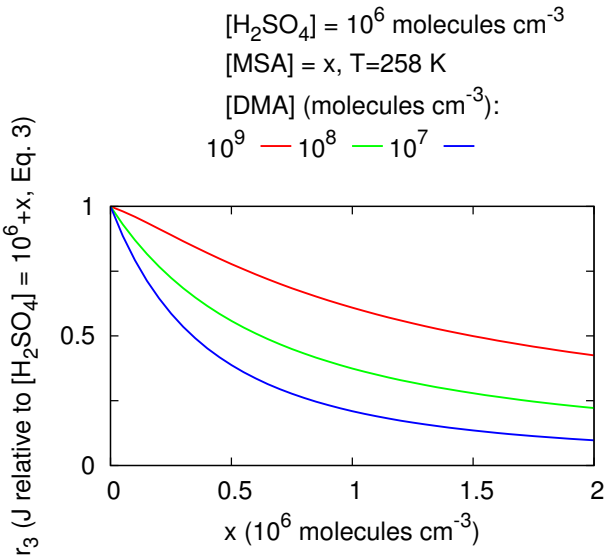

Figure 3. Cluster formation rate of added MSA relative to the same amount of added H_2SO_4 as defined in Eq. (3).

We used three DMA concentrations spanning most reported marine values ($y = 10^7$, 10^8 and 10^9 molecules cm^{-3}) (see Gibb et al., 1999, and Table 4 in Ge et al., 2011). Only field data from the boundary layer are available, and the results presented here may thus not be representative of the free troposphere, if DMA concentrations turn out to be very different from those of the boundary layer.

The resulting values for r_1 are shown in Fig. S2. In all the cases, we find that this ratio is less than 10^{-2} and, as expected, we conclude that binary MSA- and DMA-based cluster formation is of minor importance under normal conditions.

The main objective of this study is to investigate the errors of neglecting MSA as a source of condensible vapour, as this is the case in most present aerosol formation parameterisations and models. A suitable measure for this is the ratio

$$r_2 = \frac{J([\mathrm{H_2SO_4}] = 10^6,\ [\mathrm{MSA}] = x,\ [\mathrm{DMA}] = y)}{J([\mathrm{H_2SO_4}] = 10^6,\ [\mathrm{MSA}] = 0,\ [\mathrm{DMA}] = y)}, \qquad (2)$$

where J denotes the cluster formation rate at the indicated MSA concentration on top of a representative H_2SO_4 concentration, here chosen to be 10^6 molecules cm^{-3}. All other parameters are as defined above. r_2 is shown in Fig. 2 as a function of [MSA].

As expected, both temperature and DMA concentrations are important parameters for the ratio, r_2. At lower temperatures, entropy effects are decreased, and all binding free energies are more negative. In this case, the cluster growth becomes increasingly insensitive to the chemical nature of the colliding species and more dependent on the collision frequency. At high DMA levels, DMA is in large excess compared to H_2SO_4, and cluster growth is thus limited by acid collisions. In this case, having an extra source of acid has a larger effect than at lower DMA concentrations, where the DMA excess is less severe. The approximately linear dependence of r_2 on the MSA concentration could indicate that only a single MSA molecule participates at these cluster sizes. This will be investigated further in Sect. 3.3.

Adding a small amount of MSA has a small effect on the cluster formation rate, but at locations where approximately equimolar amounts of MSA and H_2SO_4 are present, this added MSA increases the cluster formation rate by ca. 15 % at 298 K, by ca. 100 % at 278 K, but by more than 300 % at 258 K in the case of [DMA] = 10^9 molecules cm^{-3}. Recalling the discussion in Sect. 2.1, and taking the latter case as an example, this increase may, however, be as small as 200 % or as large as 500 % if the binding energies are 1 kcal mol^{-1} over- or under-estimated, respectively (Fig. S3).

We consider a final descriptive ratio, indicating the effects of an unknown concentration of MSA compared to a similar deficiency in the H_2SO_4 concentration. This is given as the ratio

$$r_3 = \frac{J([\mathrm{H_2SO_4}] = 10^6,\ [\mathrm{MSA}] = x,\ [\mathrm{DMA}] = y)}{J([\mathrm{H_2SO_4}] = 10^6 + x,\ [\mathrm{MSA}] = 0,\ [\mathrm{DMA}] = y)}, \qquad (3)$$

where J represents the cluster formation rate under the given conditions, and x represents the added/deficient concentra-

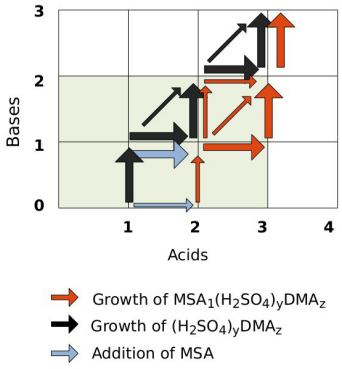

[MSA] (cm^{-3}):	10^5	10^6
Flux out:		
A_3D_2 + D	74%	34%
A_2D_2 + AD	13%	6%
A_2MD_2 + D	11%	51%
Flux to A_2MD_2:		
A_2MD	72%	71%
AMD_2	9%	9%
AMD	19%	19%
Flux to A_2D_2:		
A_2D	90%	91%
AD	10%	9%
Flux to AMD:		
AD	61%	61%
AM	39%	39%

Figure 4. Main cluster formation pathways at $T = 258\,\mathrm{K}$ and $[H_2SO_4] = 10^6$ molecules cm^{-3}, $[\mathrm{DMA}] = 10^8$ molecules cm^{-3} and two representative MSA concentrations. Dominating growth pathways are represented by thick arrows. Fluxes to clusters formed via several different pathways are indicated in the side table, where A, M and D are shorthands for H_2SO_4, MSA and DMA, respectively.

tion of MSA or H_2SO_4 in addition to a fixed H_2SO_4 concentration, again chosen to be 10^6 molecules cm^{-3}. This ratio is shown in Fig. 3 for $T = 258\,\mathrm{K}$ as function of x with the same conditions as above. This figure confirms that MSA is a less efficient clustering agent than H_2SO_4, but also that the difference is very concentration dependent. Adding a small extra amount of acid, e.g. up to 2×10^5 molecules cm^{-3}, MSA is ca. 60–90 % as efficient as a similar amount of added H_2SO_4. However, when the acid concentration is doubled from the $[H_2SO_4] = 10^6$ molecules cm^{-3} forming the reference conditions, the added MSA yields an increased cluster formation rate of ca. 20–60 % compared to the same amount of added H_2SO_4. When the acid concentration is tripled, the enhancement is ca. 10–40 %. See Figs. S4 and S5 for the corresponding plots of $T = 278\,\mathrm{K}$ and $T = 298\,\mathrm{K}$.

3.3 Growth paths

The ACDC model was used to track the main growth pathways of the clusters growing out of the simulation system. As shown in Fig. 4, the flux through the system proceeds principally via two clustering mechanisms: one that involves pure H_2SO_4–DMA clusters, and another one where the clusters contain one MSA molecule in addition to H_2SO_4 and DMA. Clusters containing more than one MSA molecule were not found to contribute significantly to the growth. The relative contribution of the two growth mechanisms to the flux out of the system depends on the concentrations of the different species; at a higher MSA concentration, the contribution of MSA-containing clusters is more prominent, as can be expected. In the case of $[\mathrm{DMA}] = 10^8$ molecules cm^{-3}, between ca. 11 and ca. 51 % of the clusters growing out of the simulation box contains one MSA molecule at $[\mathrm{MSA}] = 10^5$ molecules cm^{-3} and $[\mathrm{MSA}] = 10^6$ molecules cm^{-3} (Fig. 4). Since such clusters contain three acid molecules (H_2SO_4 or MSA), this implies overall MSA / H_2SO_4 ratios of 3 % and 17 % under these conditions.

The growth of pure H_2SO_4–DMA clusters begins with the formation of the $H_2SO_4 \cdot \mathrm{DMA}$ heterodimer, whereas the first step on the MSA–H_2SO_4–DMA growth route is the $\mathrm{MSA} \cdot H_2SO_4$ complex or the $\mathrm{MSA} \cdot H_2SO_4 \cdot \mathrm{DMA}$ cluster, formed by collision of MSA and $H_2SO_4 \cdot \mathrm{DMA}$. This is understandable, as $H_2SO_4 \cdot \mathrm{DMA}$ and $\mathrm{MSA} \cdot H_2SO_4$ are the two most stable dimers that can form in the system (Table 2). After the formation of the initial complex, the growth proceeds through subsequent collisions with H_2SO_4 and DMA molecules, but also with $H_2SO_4 \cdot \mathrm{DMA}$ dimers that are bound strongly enough to exist in notable amounts. In the MSA–H_2SO_4–DMA system, the $H_2SO_4 \cdot \mathrm{DMA}$ dimers contribute up to approximately 15 % of the H_2SO_4 concentration measurable by CIMS (i.e. clusters consisting of one H_2SO_4 and zero or more DMA molecules) under the conditions of Fig. 4, whereas $\mathrm{MSA} \cdot \mathrm{DMA}$ dimer concentrations, on the other hand, are negligible.

4 Conclusions

Methane sulfonic acid (MSA) is found in considerable quantities in the gas and aerosol phases over oceans and in coastal regions. We have investigated the effect and role of MSA in the formation of molecular clusters in atmospheres containing various quantities of MSA, H_2SO_4 and dimethyl amine (DMA). We use the Atmospheric Cluster Dynamics Code kinetic model and quantum chemical calculations of clusters containing up to three acids (MSA and/or H_2SO_4) and two DMA molecules.

In accordance with numerous previous studies, we confirm that MSA is a less potent clustering agent than H_2SO_4, but far from negligible under normal conditions. The effect of MSA depends on both the temperature and concentrations of MSA and DMA, but we find that enhancements of binary H_2SO_4–DMA-based cluster formation between 15 and 300 % are typical in the marine lower to middle troposphere.

We analyse these findings by tracking the main growth paths. We find that, at most, a single MSA is present in the growing clusters under the conditions investigated here and that, typically, MSA / H_2SO_4 ratios are below ca. 15 % at these cluster sizes. Using this model, we are thus unable to explain the MSA / H_2SO_4 ratios of up to 30 % observed by Ayers et al. (1991), Huebert et al. (1996) and Kerminen et al. (1997) in small aerosol particles. This strengthens the hypotheses that surface oxidation of DMSO or MSIA is the major source of particulate MSA (Davis et al., 1998; Barnes et al., 2006). However, we have shown that MSA may enter the aerosol particle at the earliest possible stage and significantly assist in cluster formation.

This is a consequence of MSA being a strong acid, binding strongly to DMA and H_2SO_4, and that DMA at most pristine oceanic locations is in large excess compared to acid. For actual predictions of nanometre-sized aerosol formation rates, larger clusters than the three acid–two base clusters studied here must be included in the kinetic model.

The Supplement related to this article is available online at doi:10.5194/acp-14-12023-2014-supplement.

Acknowledgements. We thank Theo Kurtén for valuable suggestions and references. We thank the European Research Council (project 257360-MOCAPAF), the Academy of Finland Center of Excellence (project 272041) and the Villum Foundation for funding. We thank the CSC Centre for Scientific Computing (Finland) and the DCSC Danish Centre for Scientific Computing for computational resources.

Edited by: M. C. Facchini

References

Almeida, J., Schobesberger, S., Kürten, A., Ortega, I. K., Kupiainen-Määttá, O., Praplan, A. P., Adamov, A., Amorim, A., Bianchi, F., Breitenlechner, M., David, A., Dommen, J., Donahue, N. M., Downard, A., Dunne, E., Duplissy, J., Ehrhart, S., Flagan, R. C., Franchin, A., Guida, R., Hakala, J., Hansel, A., Heinritzi, M., Henschel, H., Jokinen, T., Junninen, H., Kajos, M., Kangasluoma, J., Keskinen, H., Kupc, A., Kurtén, T., Kvashin, A. N., Laaksonen, A., Lehtipalo, K., Leiminger, M., Leppä, J., Loukonen, V., Makhmutov, V., Mathot, S., McGrath, M. J., Nieminen, T., Olenius, T., Onnela, A., Petäjä, T., Riccobono, F., Riipinen, I., Rissanen, M., Rondo, L., Ruuskanen, T., Santos, F. D., Sarnela, N., Schallhart, S., Schnitzhofer, R., Seinfeld, J. H., Simon, M., Sipilä, M., Stozhkov, Y., Stratmann, F., Tomé, A., Tröstl, J., Tsagkogeorgas, G., Vaattovaara, P., Viisanen, Y., Virtanen, A., Vrtala, A., Wagner,, P. E., Weingartner, E., Wex, H., Williamson, C., Wimmer, D., Ye, P., Yli-Juuti, T., Carslaw, K. S., Kulmala, M., Curtius, J., Baltensperger, U., Worsnop, D. R., Vehkamäki, H., and Kirkby, J.: Molecular understanding of sulphuric acid-amine particle nucleation in the atmosphere, Nature, 502, 359–363, 2013.

Ayers, G., Ivey, J., and Gillett, R.: Coherence between seasonal cycles of dimethyl sulphide, methanesulphonate and sulphate in marine air, Nature, 349, 404–406, 1991.

Barnes, I., Hjorth, J., and Mihalopoulos, N.: Dimethyl Sulfide and Dimethyl Sulfoxide and Their Oxidation in the Atmosphere, Chem. Rev., 106, 940–975, 2006.

Berresheim, H., Elste, T., Tremmel, H. G., Allen, A. G., Hansson, H.-C., Rosman, K., Dal Maso, M., Mäkelä, J. M., Kulmala, M., and O'Dowd, C. D.: Gas-aerosol relationships of H_2SO_4, MSA, and OH: observations in the coastal marine boundary layer at Mace Head, Ireland, J. Geophys. Res., 107, 8100, doi:10.1029/2000JD000229, 2002.

Bork, N., Kurtén, T., Enghoff, M. B., Pedersen, J. O. P., Mikkelsen, K. V., and Svensmark, H.: Ab initio studies of $O_2^-(H_2O)_n$ and $O_3^-(H_2O)_n$ anionic molecular clusters, $n \leq 12$, Atmos. Chem. Phys., 11, 7133–7142, doi:10.5194/acp-11-7133-2011, 2011.

Bork, N., Loukonen, V., and Vehkamaki, H.: Reactions and reaction rate of atmospheric SO_2 and $O_3^-(H_2O)_n$ collisions via molecular dynamics simulations, J. Phys. Chem. A, 117, 3143–3148, 2013.

Bork, N., Du, L., and Kjaergaard, H. G.: Identification and characterization of the HCl-DMS gas phase molecular complex via infrared spectroscopy and electronic structure calculations, J. Phys. Chem. A, 118, 1384–1389, doi:10.1021/jp411567x, 2014.

Bork, N., Du, L., Reiman, H., Kurtén, T. and Kjaergaard, H. G.: Benchmarking Ab Initio Binding Energies of Hydrogen-Bonded Molecular Clusters Based on FTIR Spectroscopy, J. Phys. Chem. A, 118, 5316–5322, doi:10.1021/jp5037537, 2014.

Bzdek, B. R., Ridge, D. P., and Johnston, M. V.: Reactivity of methanesulfonic acid salt clusters relevant to marine air, J. Geophys. Res.-Atmos., 116, D03301, doi:10.1029/2010JD015217, 2011.

Clark, T., Chandrasekhar, J., Spitznagel, G. W., and Schleyer, P. V. R.: Efficient diffuse function-augmented basis sets for anion calculations. III. The 3-21+G basis set for first-row elements, Li–F, J. Comput. Chem., 4, 294–301, 1983.

Dal Maso, M., Hyvärinen, A., Komppula, M., Tunved, P., Kerminen, V., Lihavainen, H., Viisanen, Y., Hansson, H.-C., and Kulmala, M.: Annual and interannual variation in boreal forest aerosol particle number and volume concentration and their connection to particle formation, Tellus B, 60, 495–508, 2008.

Dall'Osto, M., Ceburnis, D., Monahan, C., Worsnop, D. R., Bialek, J., Kulmala, M., Kurtén, T., Ehn, M., Wenger, J., Sodeau, J., Healy, R., and O'Dowd, C.: Nitrogenated and aliphatic organic vapors as possible drivers for marine secondary organic aerosol growth, J. Geophys. Res.-Atmos., 117, D12311, doi:10.1029/2012JD017522, 2012.

Davis, D., Chen, G., Kasibhatla, P., Jefferson, A., Tanner, D., Eisele, F., Lenschow, D., Neff, W., and Berresheim, H.: DMS oxidation in the Antarctic marine boundary layer: comparison of model simulations and held observations of DMS, DMSO, $DMSO_2$, H_2SO_4 (g), MSA (g), and MSA (p), J. Geophys. Res.-Atmos., 103, 1657–1678, 1998.

Dawson, M. L., Varner, M. E., Perraud, V., Ezell, M. J., Gerber, R. B., and Finlayson-Pitts, B. J.: Simplified mechanism for new particle formation from methanesulfonic acid, amines, and water via experiments and ab initio calculations, P. Natl. Acad. Sci. USA, 109, 18719–18724, 2012.

Dawson, M. L., Varner, M. E., Perraud, V., Ezell, M. J., Wilson, J., Zellenyuk, A., Gerber, R. B., and Finlayson-Pitts, B. J.: Amineâ "Amine Exchange in Aminiuâ" Methanesulfonate Aerosols, J. Phys. Chem. C, doi:10.1021/jp506560w, 2014.

Elm, J., Bilde, M., and Mikkelsen, K. V.: Assessment of density functional theory in predicting structures and free energies of reaction of atmospheric prenucleation clusters, J. Chem. Theory Comput., 8, 2071–2077, 2012.

Elm, J., Bilde, M., and Mikkelsen, K. V.: Influence of nucleation precursors on the reaction kinetics of methanol with the OH radical, J. Phys. Chem. A, 117, 6695–6701, 2013a.

Elm, J., Bilde, M., and Mikkelsen, K. V.: Assessment of binding energies of atmospherically relevant clusters, Phys. Chem. Chem. Phys., 15, 16442–16445, 2013b.

Elm, J., Fard, M., Bilde, M., and Mikkelsen, K. V.: Interaction of glycine with common atmospheric nucleation precursors, J. Phys. Chem. A, 117, 12990–12997, 2013c.

Facchini, M. C., Decesari, S., Rinaldi, M., Carbone, C., Finessi, E., Mircea, M., Fuzzi, S., Moretti, F., Tagliavini, E., Ceburnis, D., and O'Dowd, C. D.: Important source of marine secondary organic aerosol from biogenic amines, Environ. Sci. Technol., 42, 9116–9121, 2008.

Francl, M. M., Pietro, W. J., Hehre, W. J., Binkley, J. S., Gordon, M. S., DeFrees, D. J., and Pople, J. A.: Self-consistent molecular orbital methods. XXIII. A polarization-type basis set for second-row elements, J. Chem. Phys., 77, 3654–3665, 1982.

Ge, X., Wexler, A. S., and Clegg, S. L.: Atmospheric amines – Part I. A review, Atmos. Environ., 45, 524–546, 2011.

Gibb, S. W., Mantoura, R. F. C., and Liss, P. S.: Ocean-atmosphere exchange and atmospheric speciation of ammonia and methylamines in the region of the NW Arabian Sea, Global Biogeochem. Cy., 13, 161–178, 1999.

Henschel, H., Navarro, J. C. A., Yli-Juuti, T., Kupiainen-Määttä, O., Olenius, T., Ortega, I. K., Clegg, S. L., Kurtén, T., Riipinen, I., and Vehkamaki, H.: Hydration of Atmospherically Relevant Molecular Clusters: Computational Chemistry and Classical Thermodynamics, J. Phys. Chem. A, 118, 2599–2611, 2014.

Herb, J., Xu, Y., Yu, F., and Nadykto, A.: Large hydrogen-bonded pre-nucleation $(HSO_4^-)(H_2SO_4)_m(H_2O)_k$ and $(HSO_4^-)(NH_3)(H_2SO_4)_m(H_2O)_k$ clusters in the Earth's atmosphere, J. Phys. Chem. A, 117, 133–152, 2012.

Huebert, B. J., Zhuang, L., Howell, S., Noone, K., and Noone, B.: Sulfate, nitrate, methanesulfonate, chloride, ammonium, and sodium measurements from ship, island, and aircraft during the Atlantic Stratocumulus Transition Experiment/Marine Aerosol Gas Exchange, J. Geophys. Res.-Atmos., 101, 4413–4423, 1996.

Kazil, J., Stier, P., Zhang, K., Quaas, J., Kinne, S., O'Donnell, D., Rast, S., Esch, M., Ferrachat, S., Lohmann, U., and Feichter, J.: Aerosol nucleation and its role for clouds and Earth's radiative forcing in the aerosol-climate model ECHAM5-HAM, Atmos. Chem. Phys., 10, 10733–10752, doi:10.5194/acp-10-10733-2010, 2010.

Kerminen, V., Aurela, M., Hillamo, R. E., and Virkkula, A.: Formation of particulate MSA: deductions from size distribution measurements in the Finnish Arctic, Tellus B, 49, 159–171, 1997.

Kupiainen-Määttä, O., Olenius, T., Kurtén, T., and Vehkamäki, H.: CIMS sulfuric acid detection efficiency enhanced by amines due to higher dipole moments: a computational study, J. Phys. Chem. A, 117, 14109–14119, 2013.

Leverentz, H. R., Siepmann, J. I., Truhlar, D. G., Loukonen, V., and Vehkamäki, H.: Energetics of atmospherically implicated clusters made of sulfuric acid, ammonia, and dimethyl amine, J. Phys. Chem. A, 117, 3819–3825, 2013.

Loukonen, V., Kurtén, T., Ortega, I. K., Vehkamäki, H., Pádua, A. A. H., Sellegri, K., and Kulmala, M.: Enhancing effect of dimethylamine in sulfuric acid nucleation in the presence of water – a computational study, Atmos. Chem. Phys., 10, 4961–4974, doi:10.5194/acp-10-4961-2010, 2010.

McGrath, M. J., Olenius, T., Ortega, I. K., Loukonen, V., Paasonen, P., Kurtén, T., Kulmala, M., and Vehkamäki, H.: Atmospheric Cluster Dynamics Code: a flexible method for solution of the birth-death equations, Atmos. Chem. Phys., 12, 2345–2355, doi:10.5194/acp-12-2345-2012, 2012.

Nadykto, A. B., Yu, F., Jakovleva, M. V., Herb, J., and Xu, Y.: Amines in the Earth's atmosphere: a density functional theory study of the thermochemistry of pre-nucleation clusters, Entropy, 13, 554–569, 2011.

Napari, I., Kulmala, M., and Vehkamaki, H.: Ternary nucleation of inorganic acids, ammonia, and water, J. Chem. Phys., 117, 8418–8425, 2002.

Olenius, T., Kupiainen-Määttä, O., Ortega, I., Kurtén, T., and Vehkamäki, H.: Free energy barrier in the growth of sulfuric acid–ammonia and sulfuric acid–dimethylamine clusters, J. Chem. Phys., 139, 084312, doi10.1063/1.4819024, 2013.

Ortega, I. K., Kupiainen, O., Kurtén, T., Olenius, T., Wilkman, O., McGrath, M. J., Loukonen, V., and Vehkamäki, H.: From quantum chemical formation free energies to evaporation rates, Atmos. Chem. Phys., 12, 225–235, doi:10.5194/acp-12-225-2012, 2012.

Pierce, J. R. and Adams, P. J.: Uncertainty in global CCN concentrations from uncertain aerosol nucleation and primary emission rates, Atmos. Chem. Phys., 9, 1339–1356, doi:10.5194/acp-9-1339-2009, 2009.

Solomon, S., Qin, D., Manning, M., Chen, Z., Marquis, M., Averyt, K. B., Tignor, M., and Miller, H. L.: IPCC, 2007: Climate Change 2007: The Physical Science Basis. Contribution of Working Group I to the fourth assessment report of the Intergovernmental Panel on Climate Change, Cambridge University Press, Cambridge United Kingdom and New York, NY, USA, 2007.

Stewart, J. J.: Optimization of parameters for semiempirical methods V: modification of NDDO approximations and application to 70 elements, J. Mol. Model., 13, 1173–1213, 2007.

Van Dingenen, R. and Raes, F.: Ternary nucleation of methane sulphonic acid, sulphuric acid and water vapour, J. Aerosol Sci., 24, 1–17, 1993.

Weber, R., Marti, J., McMurry, P., Eisele, F., Tanner, D., and Jefferson, A.: Measured atmospheric new particle formation rates: implications for nucleation mechanisms, Chem. Eng. Commun., 151, 53–64, 1996.

Wyslouzil, B., Seinfeld, J., Flagan, R., and Okuyama, K.: Binary nucleation in acid–water systems. I. Methanesulfonic acid–water, J. Chem. Phys., 94, 6827–6841, 1991.

Zhao, Y. and Truhlar, D. G.: The M06 suite of density functionals for main group thermochemistry, thermochemical kinetics, noncovalent interactions, excited states, and transition elements: two new functionals and systematic testing of four M06-class functionals and 12 other functionals, Theor. Chem. Acc., 120, 215–241, 2008.